Biotechnology and Bioengineering

WILEY

BIOTECHNOLOGY AND BIOENGINEERING

ARTICLE OPEN ACCESS

Physiology and Robustness of Yeasts Exposed to Dynamic pH and Glucose Environments

Luca Torello Pianale[1] | Luisa Blöbaum[2] | Alexander Grünberger[2,3] | Lisbeth Olsson[1]

[1]Department of Life Sciences, Industrial Biotechnology Division, Chalmers University of Technology, Gothenburg, Sweden | [2]Multiscale Bioengineering, Technical Faculty, Bielefeld University, Bielefeld, Germany | [3]Microsystems in Bioprocess Engineering, Institute of Process Engineering in Life Sciences, Karlsruhe Institute of Technology, Karlsruhe, Germany

Correspondence: Alexander Grünberger (alexander.gruenberger@kit.edu) | Lisbeth Olsson (lisbeth.olsson@chalmers.se)

Received: 19 November 2024 | **Revised:** 13 February 2025 | **Accepted:** 22 March 2025

Funding: This study was supported by the Novo Nordisk Foundation grant DISTINGUISHED INVESTIGATOR 2019 – Research within biotechnology-based synthesis & production (grant #0055044) and Chalmers' Area of Advance Energy.

Keywords: ATP | bioprocess | biosensors | dynamic environment | glycolytic flux | microfluidics | oxidative stress | robustness | *Saccharomyces cerevisiae*

ABSTRACT

Gradients negatively affect performance in large-scale bioreactors; however, they are difficult to predict at laboratory scale. Dynamic microfluidics single-cell cultivation (dMSCC) has emerged as an important tool for investigating cell behavior in rapidly changing environments. In the present study, dMSCC, biosensors of intracellular parameters, and robustness quantification were employed to investigate the physiological response of three *Saccharomyces cerevisiae* strains to substrate and pH changes every 0.75–48 min. All strains showed higher sensitivity to substrate than pH oscillations. Strain-specific intracellular responses included higher relative glycolytic flux and oxidative stress response for strains PE2 and CEN.PK113-7D, respectively. Instead, the Ethanol Red strain displayed the least heterogeneous populations and the highest robustness for multiple functions when exposed to substrate oscillations. This result could arise from a positive trade-off between ATP levels and ATP stability over time. The present study demonstrates the importance of coupling physiological responses to dynamic environments with simultaneous characterization of strains, conditions, individual regimes, and robustness analysis. All these tools are a suitable add-on to traditional evaluation and screening workflows at both laboratory and industrial scale, and can help bridge the gap between these two.

1 | Introduction

During bioprocess scale-up, a cell factory is transferred from controlled, small laboratory volumes (ranging from high-throughput plates to bench-top reactors) to large, heterogeneous industrial conditions (~100,000 L reactors) (Wehrs et al. 2019). Therefore, mimicking key conditions at a small scale during strain development is crucial to avoid setbacks due to poor growth or suboptimal titers, rates, and yields (TRY) at industrial scale (Crater and Lievense 2018). In a large-scale bioprocess, numerous and complex perturbations affect TRY metrics (Olsson et al. 2022). For example, insufficient mixing leads to gas (Baeten et al. 2020), substrate (Larsson et al. 1996), and pH (Spann et al. 2019) gradients (Lara et al. 2006; Nadal-Rey et al. 2021). Cells experience such gradients as changing environments within seconds to minutes (Haringa et al. 2018), resulting in increased metabolic costs (Minden et al. 2022), decreased productivity (Gao et al. 2016), and population heterogeneity (Delvigne and Goffin 2014). Laboratory scale-down reactors (Neubauer and Junne 2016; Takors 2012) or pulse-feeding experiments (Anane et al. 2019; Minden et al. 2022) are used to simulate dynamic environments, though their temporal resolution is limited to minutes, at best. Modeling approaches assessing metabolic regimes (Haringa et al. 2016) or predicting metabolite (Zieringer et al. 2021) and product (Haringa et al. 2018) levels offer

Luca Torello Pianale and Luisa Blöbaum contributed equally to this study.

insights into cellular responses in a large-scale fermenter. However, a priori knowledge of the microorganism (substrate saturation constant, TRY, etc.), sophisticated modeling algorithms, and computation intensity (Haringa 2023) are required.

Microfluidics allow for manipulation and control of small volumes of fluids within short time frames (Whitesides 2006). Dynamic microfluidic single-cell cultivation (dMSCC) implements media switches within a few seconds (Blöbaum et al. 2023; Täuber et al. 2020), allowing for real-time monitoring of cell growth and intracellular responses. dMSCC has been applied to study the response of *Corynebacterium glutamicum* and *Saccharomyces cerevisiae* to substrate (Henrion et al. 2023; Täuber et al. 2020) or pH (Täuber et al. 2022). A dMSCC setup and automated pipeline have been recently adapted for yeast cultivation to assess multiple oscillation frequencies simultaneously, thereby increasing throughput (Blöbaum et al. 2024). In that proof-of-concept study, a single laboratory yeast strain was investigated in 0 and 20 g/L glucose oscillations. However, investigation of multiple strains and conditions is needed to better understand common yeast physiological responses to dynamic industrial conditions.

Microorganisms for industrial applications are often selected based on overall TRY performance rather than their ability to withstand different challenges or exhibit a stable, "robust" performance (Olsson et al. 2022). Robustness (the ability of a system to maintain a stable performance) is often neglected due to lack of reliable means to measure it (Olsson et al. 2022). A recently developed robustness quantification method has revealed robust cellular functions (such as specific growth rate, ethanol yield, etc.) and performance-robustness trade-offs in *S. cerevisiae* strains exposed to extracellular stresses (Trivellin et al. 2022). Moreover, the method is highly versatile due to the mathematical implications behind the quantification method. Besides exploring the stability of functions in face of different extracellular perturbations, the robustness formula can also measure the stability of functions over time and the degree of population heterogeneity (Torello Pianale et al. 2023).

The present study applied dMSCC and robustness quantification to compare the physiological responses of three *S. cerevisiae* strains to substrate and pH dynamics over oscillation frequencies, time, and populations. Growth and morphology characterizations were coupled with intracellular measurements of ATP, glycolytic flux, and oxidative stress using fluorescent biosensors (Pianale and Olsson 2023). Overall, this study offers a novel insight into the physiological response of various yeast strains to industrially relevant dynamic environments. Importantly, it shows how physiology-robustness analysis can be instrumental in achieving more efficient strain screening, engineering, and scale-up.

2 | Results and Discussion

2.1 | Experimental Setup: Selecting Strains, Conditions, and Oscillation Frequencies

2.1.1 | Strain Selection

Three *S. cerevisiae* strains were selected for this study (Figure 1). The laboratory strain CEN.PK113-7D is widely used for physiological studies and has a background in wild and industrial strains (Nijkamp et al. 2012). Industrial strains of Ethanol Red and PE2 are used for first-generation bioethanol production (Lino et al. 2018) and have been extensively characterized (Argueso et al. 2009; Demeke et al. 2013; Pereira et al. 2014).

2.1.2 | Selection of Substrate Dynamics

Substrate gradients in bioprocesses induce different metabolic regimes (starvation, overflow-metabolism, etc.) and cellular responses. Lifeline simulations (i.e., analysis of gradients from a cell's perspective) mimicking the late stage of industrial yeast fed-batch production suggested that cells experienced substrate limitation, overflow metabolism (substrate excess) or severe starvation depending on their location in the bioreactor (Minden et al. 2022; Sarkizi Shams Hajian et al. 2020). Substrate oscillations cause osmotic stress (Devantier et al. 2005) at both excessive (> 100 g/L) or insufficient substrate concentrations (Nadal-Rey et al. 2021). In the present study, 50 g/L glucose was selected to mimic the elevated substrate content and osmotic stress of industrial operations. At the opposite end, to determine a desirable glucose-limiting concentration, CEN.PK113-7D was grown at 5 mg/L to 20 g/L glucose (Figure 2A). Eventually, 10 mg/L glucose was selected as it kept metabolic activity above the maintenance threshold (ensuring at least one doubling) and provided energy to synthesize the required biosensors.

2.1.3 | Selection of pH Conditions

Medium pH may also be subjected to oscillation in microbial cultures (Calsamiglia et al. 2002; Cortés et al. 2016) following the addition of agents and titrants (Brunner et al. 2017; Spann et al. 2019). Moreover, contamination from lactic acid bacteria is not unusual in yeast bio-productions, lowering the pH (T. O. Basso et al. 2014; Franchi et al. 2003; Makanjuola et al. 1992; Narendranath et al. 1997) and ethanol yields (Narendranath and Power 2005). CEN.PK113-7D was grown at pH 3–5 to identify suitable conditions for subsequent experiments. Cell viability remained 100% at pH 5 and 4 but dropped to 75% at pH 3.5 and below 50% at pH 3 after 8 and 16 h (Figures 2B and S1). Most cells grown at pH 3 completed only one doubling before dying (data not shown). Therefore, pH 5 was selected as the optimal condition for growth and to resemble industrial settings. Instead, pH 3.5 was chosen as the stress condition, as it was able to negatively affect yeast cells while guaranteeing growth and avoiding excessive mortality.

2.1.4 | Oscillation Frequency Selection

Previously, CEN.PK113-7D was exposed to symmetric oscillation frequencies of 1.5, 6, 12, 24, and 48 min (Blöbaum et al. 2024), that is, cells were alternately exposed to relaxing and stressing media in a repeated and uniform cycle. These frequencies affected events at different biological timescales, ranging from RNA synthesis to replication (Nguyen et al. 2021; Shamir et al. 2016). In this present study, pH and substrate, respectively, were oscillated every 0.75, 1.5, and 6 min to mimic mixing and gradients in industrial bioreactors. In large-scale bioreactors, such changes occur from seconds

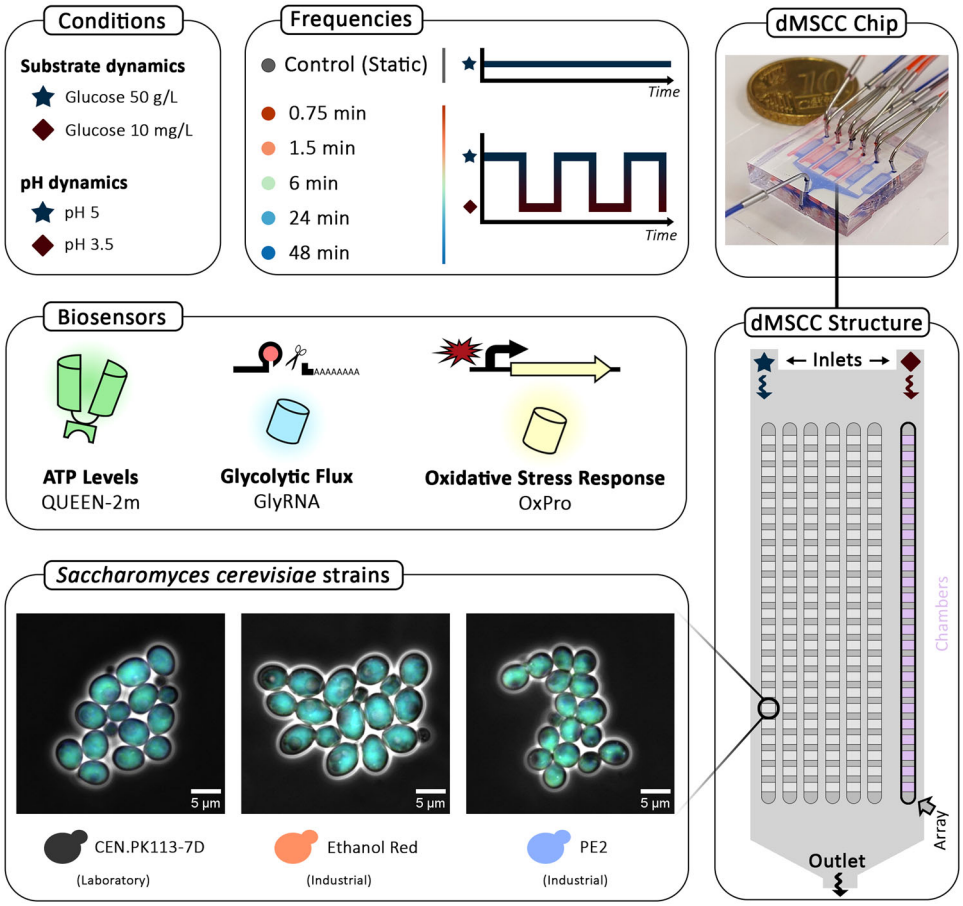

FIGURE 1 | Experimental overview of the setup. Each dMSSC chip (top right panel) is composed of six microfluidic structures (Blöbaum et al. 2024). Each oscillation structure (on the right) is composed of 6 arrays of 23 chambers for cell growth. Strains CEN.PK113-7D, Ethanol Red, and PE2 were grown in substrate and pH dynamic environments with oscillations ranging between 0.75 and 48 min. Each strain carried a biosensor for ATP levels, glycolytic flux, or oxidative stress response. The mechanism of action of biosensors is detailed in Figure 3 and in Supporting Information Text (Additional File S1).

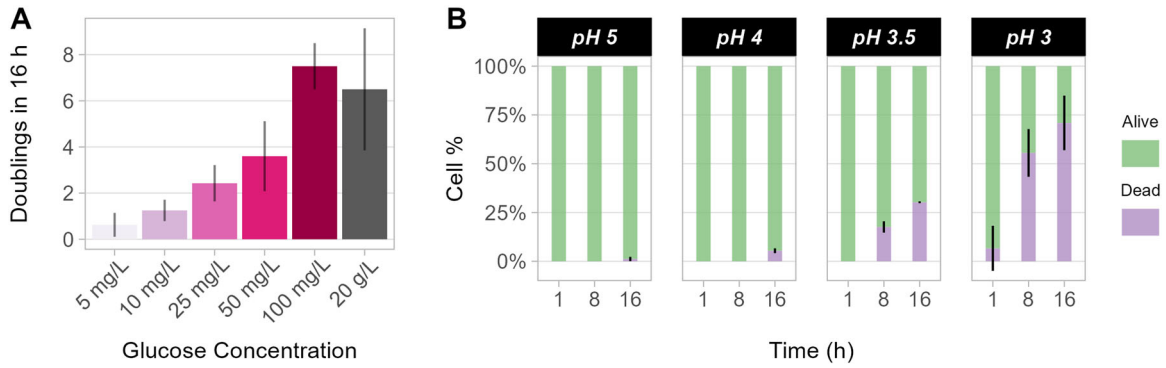

FIGURE 2 | Selection of experimental conditions. (A) Number of doublings by CEN.PK113-7D grown at different glucose concentrations ($n = 4$–8 cells across three replicates). Doublings considered the initial cells inoculated in each chamber only. (B) Percentage of alive and dead CEN.PK113-7D cells after 1, 8, and 16 h in MSCC static cultivation at various pH. Values are based on triplicates (three individual chambers) and correspond to the mean ± standard deviation.

to minutes (Haringa 2023; Haringa et al. 2017; Ho et al. 2022; Minden et al. 2022). Additionally, oscillations every 24 and 48 min were also included to assess the physiological effects of longer oscillations in the order of large-reactor mixing times (Lara et al. 2006) and their differences compared to faster oscillations (Figure 1).

Once the conditions were selected, growth (growth curves and budding ratio), morphological descriptors (cell area and circularity), and intracellular parameters (relative ATP levels, glycolytic flux, and oxidative stress response) of the selected strains were monitored using biosensors and live-cell imaging in dMSCC chips (Figures S2 and S3).

2.2 | Substrate Dynamics Have Greater Impact Than pH on Growth and Morphology

2.2.1 | Effect of Oscillating Environments on Growth

Growth was assessed as budding ratio, that is, the number of new buds per cell at any given time with respect to the previous timepoint (Equation 1) (Blöbaum et al. 2024). Ethanol Red exhibited the highest budding ratio under both substrate and pH oscillations, albeit not statistically higher compared to the other two strains (Figure 3A). The budding ratio was higher upon pH than substrate oscillations (Figures 3 and S4). *S. cerevisiae* is notoriously resistant to low pH (Carmelo et al. 1996), explaining the absence of growth impairment by any pH oscillation (Figure S5). Moreover, in the pH-dynamic setup, substrate (i.e. glucose) was not a limiting factor as it was sufficient to maintain internal homeostasis and stable growth. Previously, 24-min substrate oscillations caused the greatest reduction in budding ratio and specific growth rate (Blöbaum et al. 2024). Here, the budding ratio declined the most with oscillations of 1.5 and 6 min in CEN.PK113-7D and of 6 and 24 min in industrial strains (Figures 3B and S5). These

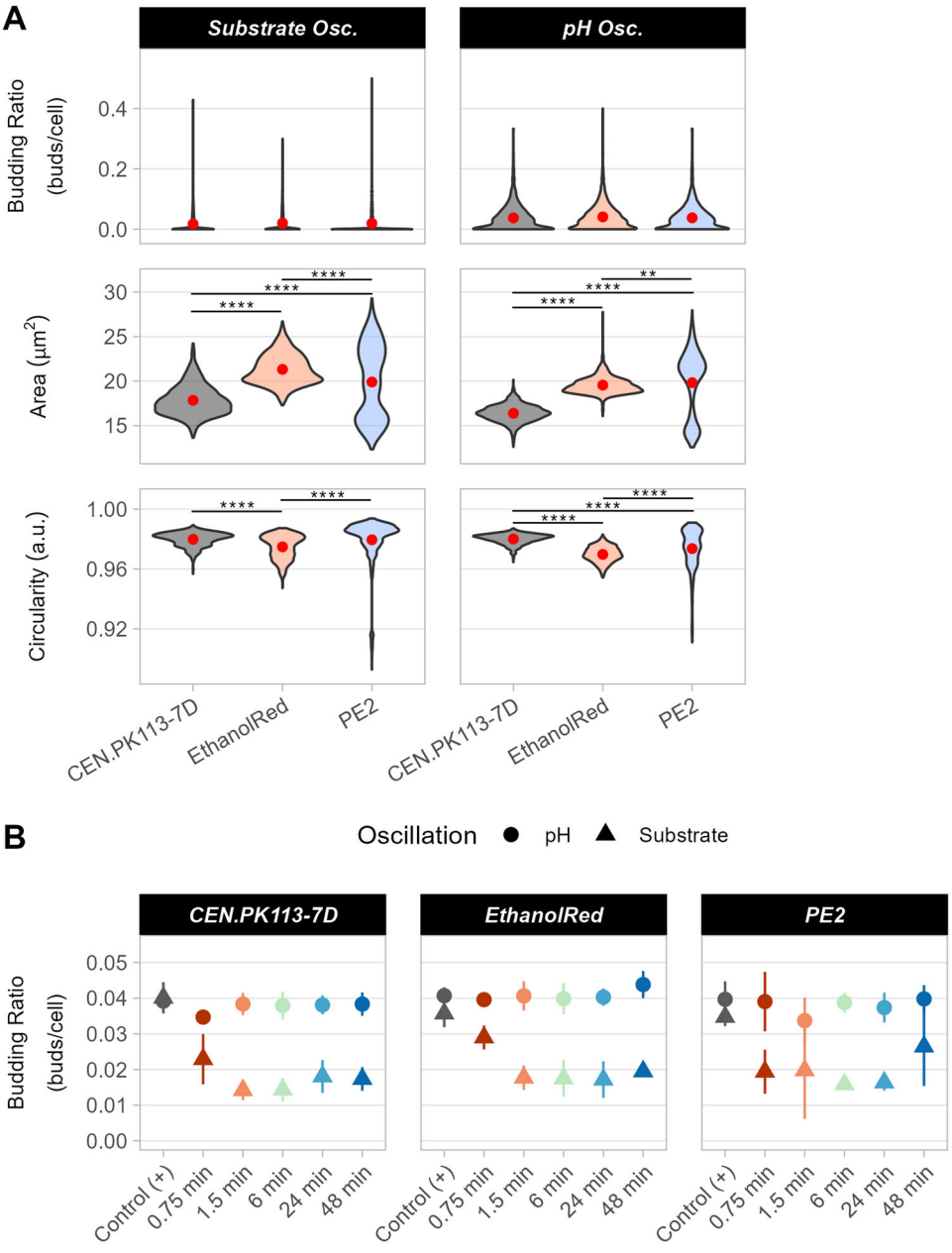

FIGURE 3 | Growth and morphology response in dynamic environments. (A) Violin plots highlight the performance of each function (budding ratio, area, and circularity) for each cell of a specific strain under all tested dynamic environments. Positive control data (static environment) are not included but are found in Figure S5. Red dots denote the mean performance across cells in all replicates and frequencies. Student's *t*-test was performed to assess differences between each pair of strains; $^{**}p \leq 0.01$, $^{****}p \leq 0.0001$. (B) Detailed overview of the budding ratio in strains exposed to substrate and pH dynamic environments and positive control (pH 5 for pH oscillations, 50 g/L glucose for substrate oscillations). Standard deviation refers to data distribution across five replicates.

differences might be due to discordant glucose concentrations: 20 and 0 g/L in the previous screening versus 50 g/L and 10 mg/L in the current one. The absence of glucose in the previous screening caused inevitably different responses compared to the present setup. More than 500 genes have been found to be differentially expressed between starving and calorie-restricted (i.e., enough substrate for metabolic activity, but not reproduction) cells (Gulli et al. 2019). The present setup better mimicked the challenges posed by large-scale processes, such as high osmotic stress caused by variations in substrate.

2.2.2 | Morphological Assessment of Yeast Cells in Oscillating Environments

Yeast morphology can be used as an indicator of cell health and can identify specific physiological states. In the brewing industry, the size and shape of yeast cells have been shown to impact fermentation efficiency and the quality of the final product, leading to off-flavors or reduced alcohol yield (Powell et al. 2003). In filamentous fungi, morphology has been shown to correlate with productivity (Wucherpfennig et al. 2011). Previous dMSCC analysis revealed feast-starvation frequency-dependant morphological changes in CEN.PK113-7D (Blöbaum et al. 2024). Here, two morphological parameters, namely cell area and circularity, were investigated in substrate and pH dynamic environments. PE2 and Ethanol Red cells were bigger than CEN.PK113-7D cells (Figures 1 and 3A), possibly due to higher ploidy (Fukuda 2023). In particular, Ethanol Red presented the biggest cells, whereas PE2 had the highest variation in cell area and circularity (Figures 3A, S2, and S3). Notably, PE2 size was the least affected by any substrate oscillation (Figures S4 and S5), although it showed a substantially higher degree of population heterogeneity in regard to cell morphology during the screenings (both as size and shape) among all the strains tested (data not shown). Overall, substrate oscillations resulted in bigger and rounder cells than pH oscillations (Figures 3A and S5). Altering the surface-to-volume ratio by changing morphology shape and size might be a strategy to regulate nutrient uptake (Turner et al. 2012). Instead, a less round and smaller phenotype in pH oscillations may result from cell wall alterations and deformations caused by low pH (de Lucena et al. 2012, 2015; Ribeiro et al. 2022).

2.3 | Fluctuating Environments Induce Strain-Specific Intracellular Parameter Responses

2.3.1 | Biosensor Selection

One advantage of using dMSCC is its combination with fluorescent biosensors to monitor the response of desired intracellular parameters in dynamic environments (Blöbaum et al. 2024). Here, the selected strains were engineered with biosensors of intracellular ATP levels, glycolytic flux, and oxidative stress response using the *Sc*EnSor Kit (Pianale and Olsson 2023) (Figure 4A and Supporting Information Text in Additional File S1). While the ATP biosensor (QUEEN-2m) had a response time of a few seconds to detect changes in ATP levels (being a circularly-permuted biosensor) (Blöbaum et al. 2024; Takaine 2019), the oxidative stress and glycolytic flux biosensor (GlyOx) had a response time in the order of tens of minutes (being based on transcription, translation, and maturation of fluorescent proteins to detect the desired parameters) (Pianale and Olsson 2023). However, these biosensors were still useful for grasping general trends in physiological behaviors through all the oscillation frequencies tested. Moreover, biosensors with response times slower than environmental oscillations are still able to spot differences as the biosensor response shifts to a new steady state (Nguyen et al. 2021). More in-depth considerations are available in the Supporting Information Text in Additional File S1. For all biosensors, relative changes to the positive control were computed using Equation 2 and represent the fold increase/decrease for each parameter (Figures S6 and S7). Some considerations should be made for these biosensors.

2.3.2 | ATP Levels and Glycolytic Flux

Relative ATP levels dropped significantly (to < 1) when cells were exposed to substrate oscillations while remaining similar to the control (~1) in pH oscillations (Figures 4B, S6, and S7). As with the budding ratio, this result can be explained by constant substrate content and, therefore, stable ATP production encountered during pH dynamics. The relative glycolytic flux was also higher during pH as opposed to substrate oscillations (Figures 4B and S7). Ethanol Red manifested significantly higher relative ATP levels than CEN.PK113-7D and PE2 in response to substrate dynamics, whereas the opposite was true for pH oscillations (Figure 4B). Ethanol Red is more resistant to substrate fluctuations and can adapt more easily to such conditions than CEN.PK113-7D (Minden et al. 2022, 2023a, 2023b), which is slower at mobilizing the storage carbon pools (mainly trehalose) (Minden et al. 2022, 2023a; Thevelein 1984), due to a mutation in the *CYR1* gene (Nijkamp et al. 2012). The greater metabolic flexibility of Ethanol Red might also be suggested by its higher relative glycolytic flux in short oscillations (0.75 and 1.5 min) compared to CEN.PK113-7D, but lower in longer ones (6 and 24 min) (Figures 4C and S6). Interestingly, PE2 was the only strain to increase the relative glycolytic flux (< 1) when exposed to both substrate and pH oscillations; while CEN.PK113-7D displayed the opposite trend (> 1) and Ethanol Red showed no difference or a slight decrease with respect to control conditions (Figure 4B). Such discrepancies might be caused by strain-specific expression or substrate affinity of hexose transporters (Maier et al. 2002; Nadai et al. 2021), or by strain-specific metabolic responses (Onetto et al. 2021; Trivellin et al. 2024). Given its tolerance of low pH (Coradini et al. 2021; Della-Bianca et al. 2014), PE2 responded better to pH oscillations in terms of ATP levels and glycolytic flux but displayed the lowest oxidative stress response (Figure 4B).

2.3.3 | Substrate Oscillations Lower the Oxidative Stress Response

Substrate oscillations dampened the oxidative stress response (< 1), particularly in CEN.PK113-7D (Figure 4B); whereas pH oscillations had comparable oxidative stress levels compared to the control condition (~1), thus causing higher relative oxidative stress response compared to substrate oscillations for all the strains (Figures 4B and S7). The observed divergence could be related to differences in respiratory metabolism or regulation by the stress-responsive transcription factor Yap1p. Reactive

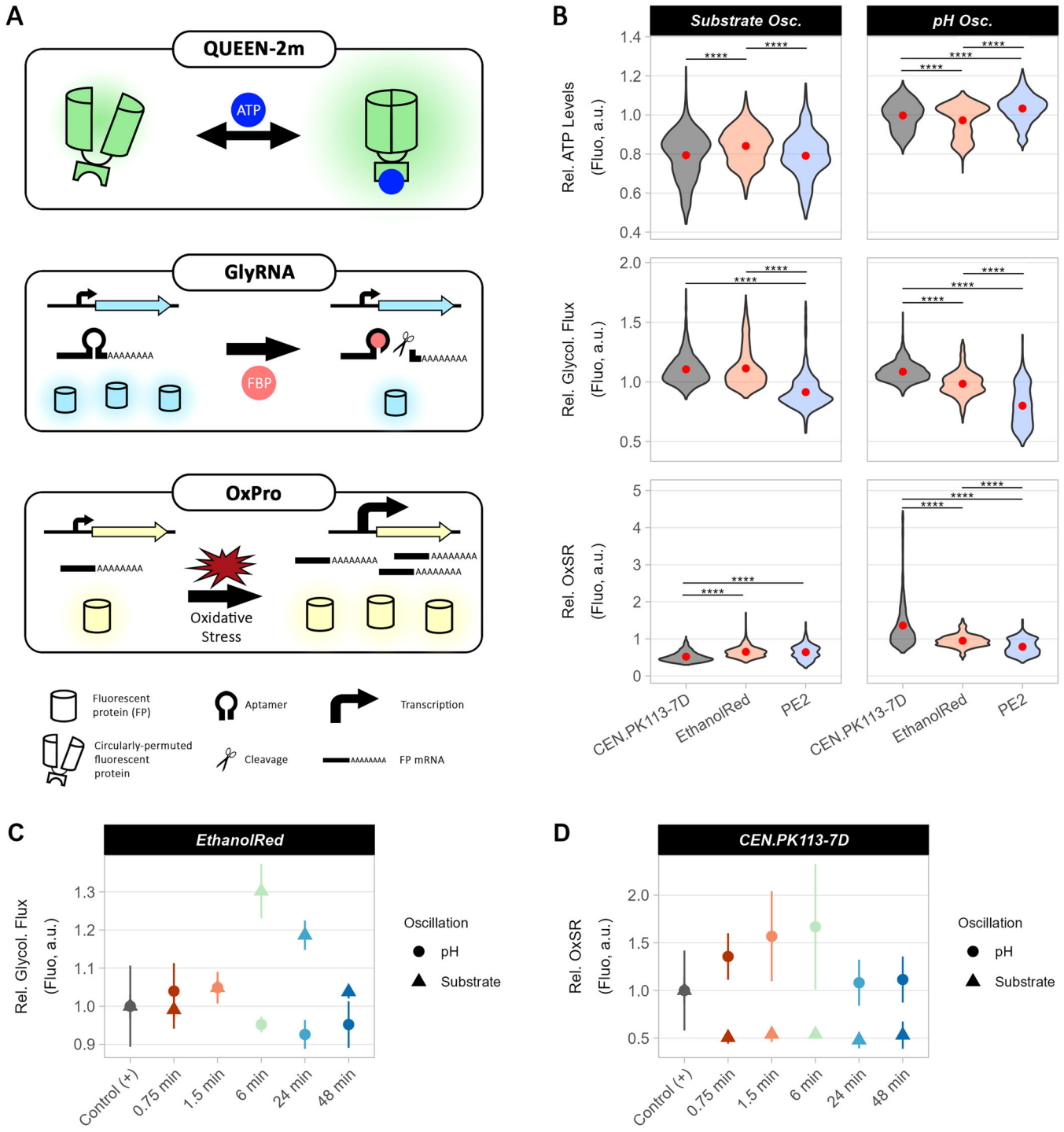

FIGURE 4 | Biosensor mode of action and response in dynamic environments. (A) Overview and mechanisms of action of biosensors for ATP (QUEEN-2m, a circularly-permuted fluorescent protein), glycolytic flux (GlyRNA, a fructose-bis-phosphate (FBP)-sensitive aptameric biosensor), and oxidative stress (OxPro, an oxidative stress-sensitive synthetic-promoter-based biosensor). (B) Relative ATP, glycolytic flux, and oxidative stress of the three selected strains upon substrate (left) and pH (right) dynamics. Violin plots highlight single-cell performance. Positive control data (static environment) are not included (see Figure S6). Red dots denote the mean performance across cells in all replicates and dynamic oscillation frequencies. Student's *t*-test was performed to assess differences between each pair of strains; $^{****}p \leq 0.0001$. (C and D) Relative glycolytic flux in Ethanol Red (C) and relative oxidative stress response in CEN.PK113-7D (D) exposed to substrate and pH dynamic environments and a static positive control (pH 5 for pH oscillations, 50 g/L glucose for substrate oscillations). Standard deviation refers to data distribution across five replicates.

oxygen species are generated during respiration. In the presence of oxygen, yeast cells have a respiro-fermentative (overflow) metabolism when the substrate is abundant and a respiratory metabolism when it is low (Pfeiffer and Morley 2014). During pH oscillations and at 50 g/L glucose in substrate oscillations, an overflow metabolism was guaranteed. Instead, 10 mg/L glucose triggered a respiratory metabolism (not necessarily at full capacity), which allowed maintenance but limited replication. This

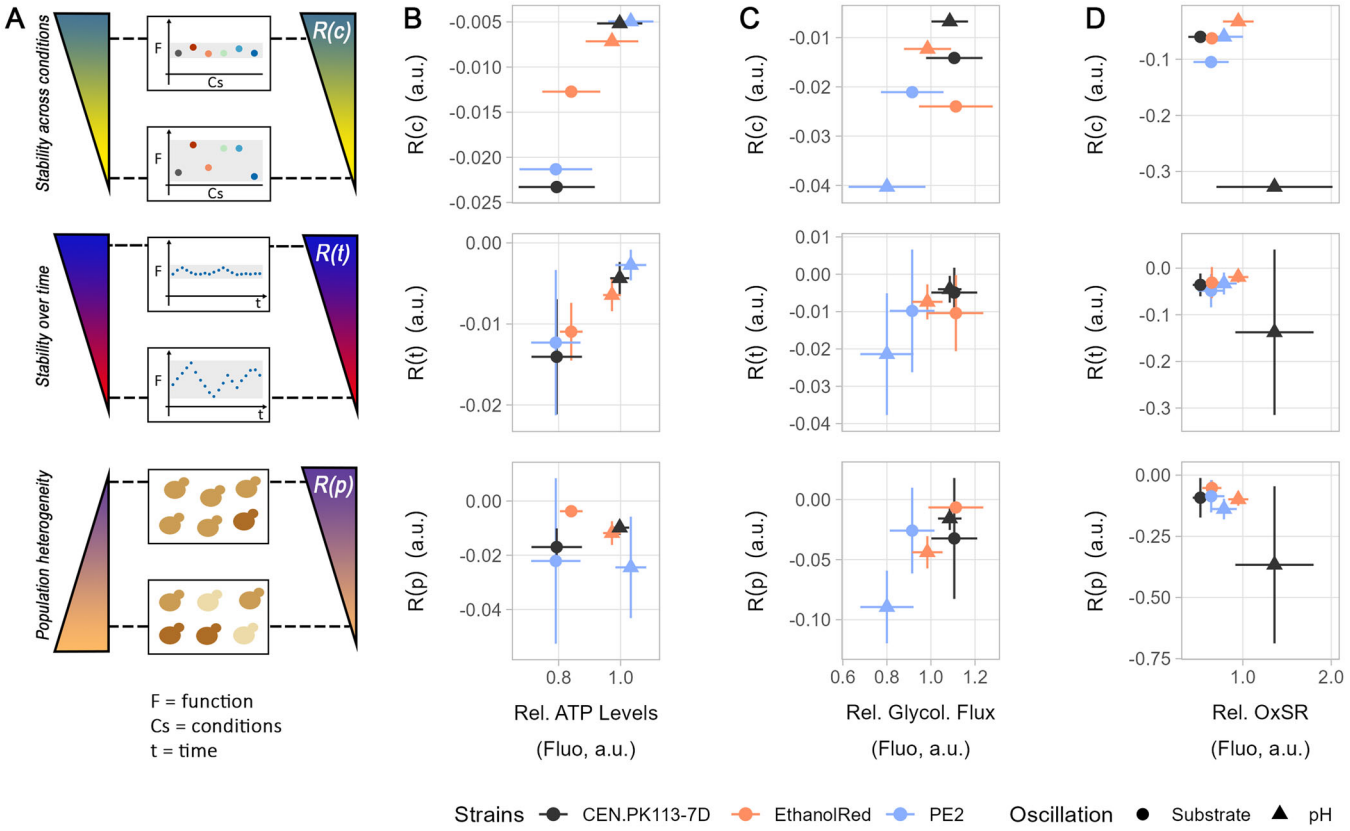

FIGURE 5 | Intracellular parameter performance and robustness relationship. (A) Visual representation of robustness types. For a desired function (e.g., ATP levels) and set of conditions (e.g., different oscillation frequencies), it is possible to use the robustness quantification method to measure the stability of a function across conditions R(c), populations R(p), and over time R(t). (B–D) Correlation between performance (*x*-axis) and robustness types (*y*-axis) for relative ATP levels (B), glycolytic flux (C), and oxidative stress response (D). For each intracellular parameter, robustness across conditions, R(c) (top), over time, R(t) (middle), and across populations, R(p) (bottom), are shown. Standard deviation represents the distribution across five oscillation frequencies only (no positive static control included) with five replicates each.

may have generated fewer reactive oxygen species and, consequently, a lower oxidative stress response. Alternatively, the discrepancy might be related to the synthesis of methylglyoxal, a toxic metabolite produced during glycolysis, which activates Yap1p and triggers the oxidative stress response (Maeta et al. 2004). A constant glucose concentration in pH oscillations might have triggered methylglyoxal synthesis and a baseline oxidative stress response. Instead, low glucose periods in substrate oscillations might have decreased methylglyoxal synthesis and the stress response. Interestingly, only in CEN.PK113-7D, pH oscillations boosted the oxidative stress response (Figure 4B), particularly at 0.75, 1.5, and 6 min (Figures 4D and S6). Activation of the oxidative stress response in laboratory strains has been documented at pH 3.5 (Kapteyn et al. 2001) and 2.5 (de Lucena et al. 2015). On the contrary, the industrial strain JP1 was shown to trigger only a general stress response at low pH (De Melo et al. 2010).

2.4 | Robustness Analysis Highlights Different Aspects of Function Stability

Robustness quantification, especially at a small laboratory scale, can facilitate the physiological characterization and selection of microorganisms for industrial purposes. Using the Fano-factor-based equation developed by Trivellin and collaborators (Trivellin et al. 2022), robustness quantification can inherently grasp and condense in a single number the dispersion of a data set, allowing for the study of function stability across different conditions, times, and populations (Blöbaum et al. 2024; Torello Pianale et al. 2023) (Figure 5A).

2.4.1 | Robustness Across Conditions

The robustness of functions over different oscillation frequencies (0.75–48 min, static control environments not included), referred to as R(c), was computed for each strain and oscillation type (pH and substrate) (Figure 5A–D, top). A higher R(c) indicates that strain performance is less affected by oscillation frequency (Figure 5A). Relative ATP levels and their R(c) were higher under pH than substrate oscillations. Overall, higher ATP levels seemed to correlate with higher R(c) (Figure 5B, top). On the one hand, PE2 displayed an increase in glycolytic flux but the lowest R(c) for this parameter (Figure 5C, top). On the other hand, CEN.PK113-7D exhibited the greatest drop in glycolytic flux but an elevated R(c), suggesting a poorly consistent reduction (Figure 5C, top).

2.4.2 | Robustness Over Time

To determine performance stability, Equation 3 can be used to compute the robustness of a function over time, referred to as

R(t). Accordingly, limited dispersion over time compared to the mean corresponds to a high R(t) (Blöbaum et al. 2024; Torello Pianale et al. 2023) (Figure 5A). Here, relative ATP levels over time were more stable in pH than substrate oscillations (Figure 5B, middle and Figure S8), in line with performance results (Figures 4B and S7). Similar to R(c), Ethanol Red achieved the highest ATP levels and corresponding R(t) in substrate oscillations, but the lowest in pH oscillations (Figure 5B, middle); whereas PE2 did so for pH oscillations (Figure 5B, middle). Longer oscillation frequencies (24 and 48 min) resulted in more stable ATP levels over time, regardless of oscillation type (Figure S9), owing to optimized energy production and usage (Thomsson et al. 2003; N. Zhang and Cao 2017). PE2 was the only strain with lower R(t) for relative glycolytic flux in pH oscillations. Interestingly, substrate oscillations stabilized the glycolytic flux over time in spite of less stable ATP levels (Figure S9). Lastly, CEN.PK113-7D exposed to pH oscillations manifested the highest increase in oxidative stress response but with the lowest stability over time (Figure 5D, middle and Figure S8A).

2.4.3 | Robustness Across Populations

Population heterogeneity arises from the existence of phenotypically diverse subpopulations within an isogenic bulk population. Phenotypic heterogeneity might be due to intrinsic (e.g., stochastic gene expression/noise) or extrinsic (e.g., gradients) factors (Gasperotti et al. 2020). Stemming from Equation 3, robustness across populations, referred to as R(p), indicates how homogeneous a function is across a population. Elevated R(p) denotes low population heterogeneity; low R(p) a higher one (Figure 5A). In dynamic environments, Ethanol Red exhibited the lowest population heterogeneity (Figures 5 and S10), echoing previous results on lignocellulosic hydrolysates (Torello Pianale et al. 2023). CEN.PK113-7D exposed to pH oscillations displayed the highest R(p) for relative glycolytic flux but the lowest R(p) for oxidative stress (Figure 5C,D, bottom and Figure S10). All strains exhibited less population heterogeneity when exposed to substrate than pH oscillations (Figure 5, bottom and Figure S10). This could be due to two factors. First, the lower impact of pH oscillations on strain performance limited the effect of extrinsic factors on population heterogeneity. Second, the reduced ability to synthesize macromolecules and scarce energy availability caused by substrate oscillations might limit the effect of intrinsic factors, as all cells would switch to "survival mode" and show less heterogeneity. The latter could be picked by transcriptome or metabolome differences, especially in log-phase growing cells (Pinheiro et al. 2022).

3 | Conclusions

In the present study, we employed dMSCC to investigate the physiological response of three yeast strains to changes in substrate and pH. Strains, conditions, and individual regimes were compared. Strain-specific trends in oscillating environments included an increased oxidative stress response in CEN.PK113-7D and increased relative glycolytic flux in PE2. Substrate oscillations appeared to be more detrimental than pH ones. Fast and slow oscillation frequencies caused distinct responses within each strain. Finally, robustness investigation confirmed Ethanol Red as a strain with low population heterogeneity and stable functions when subjected to substrate oscillations.

The detailed level of resolution in the screenings and high throughput offered by the semi-automated pipeline used might have several practical applications. For one, they may facilitate an understanding of common physiological responses to changing environments (fast or slow). This approach might be advantageous when selecting and improving industrial strains, as it offers the possibility to characterize strains based on specific requirements (performance, intracellular parameters or robustness features) in either static or dynamic environments. Such ability will help overcome the bottlenecks caused by gradients and heterogeneities encountered during scale-up.

4 | Materials and Methods

4.1 | Strains, Media and Cultivation Conditions

The *S. cerevisiae* strains used in this study were the laboratory CEN.PK113-7D (*MATa URA3 HIS3 LEU2 TRP1 MAL2-8c SUC2*) (Entian and Kötter 2007) and industrial bioethanol-producing Ethanol Red (Société Industrielle Lesaffre, Division Leaf) and PE2 (L. C. Basso et al. 2008). Biosensors monitoring intracellular ATP (Takaine 2019), glycolytic flux (Ortega et al. 2021), and oxidative stress response (J. Zhang et al. 2016) were integrated into the genome using the *Sc*EnSor kit (Pianale and Olsson 2023) (Addgene repository ID #1000000215).

Synthetic-defined minimal Verduyn ("Delft") medium was used as a base for all screenings. The medium contained 5 g/L $(NH_4)_2SO_4$, 3 g/L KH_2PO_4, 1 g/L $MgSO_4{\cdot}7H_2O$, 1 mL/L trace metal solution, and 1 mL/L vitamin solution (Torello Pianale et al. 2022). The glucose concentration and pH were adjusted based on the screening performed. In substrate oscillations, pH was adjusted to 5, and glucose was switched between 10 mg/L (stress) or 50 g/L (relaxing medium). In pH oscillations, glucose was set at 20 g/L, while pH was adjusted to 3.5 (stress) or 5 (relaxing medium).

All cultivations were performed at 30°C. Pre-cultures were inoculated with 10 µL of cells from a cryostock in 10 mL Delft medium supplemented with 50 mM succinate buffer (5.9 g/L succinic acid and 3.54 g/L NaOH) in a 100-mL baffled flask. Pre-cultures were grown for 16 h at 120 rpm (shaking throw of 25 mm), diluted to $OD_{600} = 0.3$, and added to the microfluidic chips. In the screening, cells were adapted for 4 h in a relaxing medium, followed by 12 h of symmetric oscillations at different frequencies (0.75, 1.5, 6, 12, or 48 min). A pressure-driven pump (Line-up EZ series, Fluigent) maintained the desired dynamic flow profiles of relaxing medium (100 mbar) and stress medium (70 or 220 mbar). This, in combination with the oxygen-permeable material used for the chip, guaranteed a constant presence of oxygen in the cultivation chambers avoiding oxygen limitation.

4.2 | dMSCC and Image Analysis

The dMSCC was as described previously (Blöbaum et al. 2024). Briefly, the polydimethylsiloxane (PDMS) microfluidic chips included six cultivation structures, one dedicated to the positive control (static environment, relaxing medium) and five oscillation experiments. Each structure (Figure 1A, right panel) bore 7 arrays of 23 monolayer-growth chambers, 6 were exposed to dynamic conditions and 1 was for the negative control (static environment, stressful medium). Each monolayer-growth chamber has dimensions of $4 \times 90 \times 80\,\mu m$ (height × width × length), while the channels have a height of 14 μm.

Chip fabrication followed a previously reported protocol (Blöbaum et al. 2023). The microfluidic chip was molded from a silicon wafer. Inlets and outlets connecting media were punched using a biopsy puncher. The PDMS chip and the glass slide were cleaned with isopropanol and activated in a plasma oven. The activated surfaces bonded upon contact.

For live-cell imaging, the chip was positioned on an inverted automated microscope (Nikon Eclipse Ti2) equipped with an LED-based light source for episcopic fluorescence (Sola SE II Set, Lumencor) and a 100 × oil objective (CFI P-Apo DM Lambda, Nikon). The temperature in the incubator cage (OKO-H201, OKO Lab) was kept at 30°C. Phase-contrast and fluorescent images (see acquisition settings in Table 1) were captured every 8 or 10 min for QUEEN-2m or GlyOx biosensors, respectively.

A previously published pipeline (Blöbaum et al. 2024) based on Fiji (Schindelin et al. 2012) was used for image handling and analysis. Briefly, an image pre-processing step was used to load, stabilize, tilt, and cut the images. Next, rolling ball background subtraction was performed to allow optimal fluorescence quantification. Yeast cell segmentation was performed using the trained model "Yeast_Segmentation_v2.2" (available via GitHub, github.com/lucatorep/Robustness_Microfluidics), a StarDist 2D model (Schmidt et al. 2018) previously trained using the StarDist 2D ZeroCostDL4Mic notebook (von Chamier et al. 2021), and an augmentor algorithm (Bloice et al. 2017). Finally, fluorescent quantification and morphological analysis of yeast cells were performed.

4.3 | Data and Statistical Analysis

Data and statistical analysis were carried out in R (R Core Team 2020). Statistical significance was defined as follows: $*p \leq 0.05$, $**p \leq 0.01$, $***p \leq 0.001$, and $****p \leq 0.0001$.

The budding ratio was used to quantify growth of strains in dMSCC chips according to Equation 1 (Blöbaum et al. 2024).

$$\text{Budding ratio} = \frac{(\text{no. buds})_{t(n)}}{(\text{no. cells})_{t(n-1)}}. \quad (1)$$

Here, the number of new buds at a given time point "n" was divided by the number of cells at the previous time point "$n-1$."

Biosensor output for each strain was computed as a ratio between uvGFP and GFP for QUEEN-2m, CFP and RFP for GlyRNA, and YFP and RFP for OxPro (Blöbaum et al. 2024; Pianale and Olsson 2023; Torello Pianale et al. 2022). Subsequently, the relative intracellular parameter computations were carried out using Equation 2.

$$\text{Relative intracellular parameter}_{t(n)} = \frac{Fluo_{t(n)}}{\overline{Fluo}_{PC}}. \quad (2)$$

Here, each fluorescence ratio at any given timepoint, $Fluo_{t(n)}$, is divided by the overall mean fluorescence ratio of the positive control during the 12 h of screening, $Fluo_{PC}$. This allows comparison without constructing calibration curves for each strain and biosensor.

Robustness was quantified using Equation 3 (Trivellin et al. 2022).

$$R = -\frac{\sigma^2}{\bar{x}} \times \frac{1}{m}. \quad (3)$$

When computing R(c), σ and x refer to the standard deviation and mean (respectively) of a function (relative ATP levels, glycolytic flux, and oxidative stress response) across multiple oscillation frequencies (each in five replicates) for one single strain; while m refers to the mean of a function across all conditions and strains. Therefore, R(c) identifies how stable a

TABLE 1 | Filter details and setup used in this study.

Channel	Excitation wavelength (nm)	DM (nm)	Emission wavelength (nm)	Filter brand	Exposure (ms)	Intensity (%)
Phase contrast	—	—	—	—	100	15–25
RFP[a]	562/40	593	640/75	Nikon	60	10
YFP[a]	500/24	520	542/27	Nikon	100	10
GFP[b]	472/30	495	520/35	Nikon	400	25
CFP[a]	420/40x	455	470 Long Pass	Custom	80	10
uvGFP[b]	390/40	425	520/35	AHF	800	25

[a]Required for GlyOx.
[b]Required for QUEEN-2m.

function is in the face of different oscillation frequencies for each strain.

When computing R(t), σ and x refer to the standard deviation and mean (respectively) of the biosensor signal output (function) throughout the screening for each strain replicate in each oscillation frequency replicate; while m refers to the mean of a function across all strains. Therefore, R(t) identifies how stable a function is over time in each oscillation frequency.

When computing R(p), σ and x refer to the standard deviation and mean, respectively, of a function (relative ATP levels, glycolytic flux, and oxidative stress response) across all cells at each time point of a condition; while m refers to the mean of a function across all time points and conditions. Therefore, R(p) describes how homogeneous a function is across a cell population.

A visual representation of data analysis pipelines and a description of the concepts used can be found in our previous publications (Blöbaum et al. 2024; Torello Pianale et al. 2023).

Author Contributions

L.T.P. and L.B. conceived the study and performed the experiments. L.T.P. performed data analysis. L.T.P. and L.B. wrote the manuscript. L.O. and A.G. supervised and contributed to the discussion of collected data. All authors contributed to the correction of the manuscript before submission.

Acknowledgments

The *Saccharomyces cerevisiae* Ethanol Red strain was kindly provided by Société Industrielle Lesaffre, Division Leaf. We thank Cecilia Trivellin and Nathalia Vilela for fruitful discussions and Nika Erjavec for linguistic correction of the manuscript. We thank the Department of Biophysics and Nanoscience, as well as the Department for Physics of Supramolecular Systems and Surfaces at Bielefeld University, for giving access and support to their clean room facilities. L.B. was supported by the Joachim-Herz-Foundation (Add-on Fellowship for interdisciplinary Life Sciences). Novo Nordisk Foundation grant DISTINGUISHED INVESTIGATOR 2019 – Research within biotechnology-based synthesis & production (grant #0055044) supported the present study. Chalmers' Area of Advance Energy supported L.T.P. with a travel grant to perform the experiments at Bielefeld University with L.B.

Conflicts of Interest

The authors declare no conflicts of interest.

Data Availability Statement

The data sets generated and/or analyzed during the current study are available from the corresponding author upon reasonable request.

References

Anane, E., Á. C. García, B. Haby, et al. 2019. "A Model-Based Framework for Parallel Scale-Down Fed-Batch Cultivations in Mini-Bioreactors for Accelerated Phenotyping." *Biotechnology and Bioengineering* 116, no. 11: 2906–2918. https://doi.org/10.1002/BIT.27116.

Argueso, J. L., M. F. Carazzolle, P. A. Mieczkowski, et al. 2009. "Genome Structure of a *Saccharomyces cerevisiae* Strain Widely Used in Bioethanol Production." *Genome Research* 19, no. 12: 2258–2270. https://doi.org/10.1101/GR.091777.109.

Baeten, J. E., M. C. M. van Loosdrecht, and E. I. P. Volcke. 2020. "When and Why Do Gradients of the Gas Phase Composition and Pressure Affect Liquid-Gas Transfer?" *Water Research* 178: 115844. https://doi.org/10.1016/J.WATRES.2020.115844.

Basso, L. C., H. V. De Amorim, A. J. De Oliveira, and M. L. Lopes. 2008. "Yeast Selection for Fuel Ethanol Production in Brazil." *FEMS Yeast Research* 8: 1155–1163. https://doi.org/10.1111/j.1567-1364.2008.00428.x.

Basso, T. O., F. S. Gomes, M. L. Lopes, H. V. De Amorim, G. Eggleston, and L. C. Basso. 2014. "Homo- and Heterofermentative Lactobacilli Differently Affect Sugarcane-Based Fuel Ethanol Fermentation." *Antonie Van Leeuwenhoek* 105, no. 1: 169–177. https://doi.org/10.1007/S10482-013-0063-6.

Blöbaum, L., S. Täuber, and A. Grünberger. 2023. "Protocol to Perform Dynamic Microfluidic Single-Cell Cultivation of *C. glutamicum*." *STAR Protocols* 4, no. 3: 102436. https://doi.org/10.1016/J.XPRO.2023.102436.

Blöbaum, L., L. Torello Pianale, L. Olsson, and A. Grünberger. 2024. "Quantifying Microbial Robustness in Dynamic Environments Using Microfluidic Single-Cell Cultivation." *Microbial Cell Factories* 23, no. 1: 44. https://doi.org/10.1186/S12934-024-02318-Z.

Bloice, M. D., C. Stocker, and A. Holzinger. 2017. "Augmentor: An Image Augmentation Library for Machine Learning." *Journal of Open Source Software* 2, no. 19: 432. https://doi.org/10.21105/JOSS.00432.

Brunner, M., P. Braun, P. Doppler, et al. 2017. "The Impact of pH Inhomogeneities on CHO Cell Physiology and Fed-Batch Process Performance – Two-Compartment Scale-Down Modelling and Intracellular pH Excursion." *Biotechnology Journal* 12, no. 7: 1600633. https://doi.org/10.1002/BIOT.201600633.

Calsamiglia, S., A. Ferret, and M. Devant. 2002. "Effects of pH and pH Fluctuations on Microbial Fermentation and Nutrient Flow From a Dual-Flow Continuous Culture System." *Journal of Dairy Science* 85, no. 3: 574–579. https://doi.org/10.3168/JDS.S0022-0302(02)74111-8.

Carmelo, V., P. Bogaerts, and I. Sá-Correia. 1996. "Activity of Plasma Membrane H+-Atpase and Expression of *PMA1* and *PMA2* Genes in *Saccharomyces cerevisiae* Cells Grown at Optimal and Low pH." *Archives of Microbiology* 166, no. 5: 315–320. https://doi.org/10.1007/S002030050389/METRICS.

Coradini, A. L. V., F. da Silveira Bezerra de Mello, M. Furlan, et al. 2021. "QTL Mapping of a Brazilian Bioethanol Strain Links the Cell Wall Protein-Encoding Gene *GAS1* to Low pH Tolerance in *S. cerevisiae*." *Biotechnology for Biofuels* 14, no. 1: 239. https://doi.org/10.1186/S13068-021-02079-6.

Cortés, J. T., N. Flores, F. Bolívar, A. R. Lara, and O. T. Ramírez. 2016. "Physiological Effects of pH Gradients on *Escherichia coli* During Plasmid DNA Production." *Biotechnology and Bioengineering* 113, no. 3: 598–611. https://doi.org/10.1002/BIT.25817.

Crater, J. S., and J. C. Lievense. 2018. "Scale-Up of Industrial Microbial Processes." *FEMS Microbiology Letters* 365, no. 13: 138. https://doi.org/10.1093/FEMSLE/FNY138.

Della-Bianca, B. E., E. de Hulster, J. T. Pronk, A. J. A. van Maris, and A. K. Gombert. 2014. "Physiology of the Fuel Ethanol Strain *Saccharomyces cerevisiae* PE-2 at Low pH Indicates a Context-Dependent Performance Relevant for Industrial Applications." *FEMS Yeast Research* 14, no. 8: 1196–1205. https://doi.org/10.1111/1567-1364.12217.

de Lucena, R. M., C. Elsztein, W. de Barros Pita, R. B. de Souza, S. de Sá Leitão Paiva Júnior, and M. A. de Morais Junior. 2015. "Transcriptomic Response of *Saccharomyces cerevisiae* for Its Adaptation to Sulphuric Acid-Induced Stress." *Antonie Van Leeuwenhoek* 108, no. 5: 1147–1160. https://doi.org/10.1007/S10482-015-0568-2.

de Lucena, R. M., C. Elsztein, D. A. Simões, and M. A. Morais. 2012. "Participation of CWI, HOG and Calcineurin Pathways in the Tolerance of *Saccharomyces cerevisiae* to Low pH by Inorganic Acid." *Journal of Applied Microbiology* 113, no. 3: 629–640. https://doi.org/10.1111/J.1365-2672.2012.05362.X.

Delvigne, F., and P. Goffin. 2014. "Microbial Heterogeneity Affects Bioprocess Robustness: Dynamic Single-Cell Analysis Contributes to Understanding of Microbial Populations." *Biotechnology Journal* 9, no. 1: 61–72. https://doi.org/10.1002/BIOT.201300119.

Demeke, M. M., H. Dietz, Y. Li, et al. 2013. "Development of a D-Xylose Fermenting and Inhibitor Tolerant Industrial *Saccharomyces cerevisiae* Strain With High Performance in Lignocellulose Hydrolysates Using Metabolic and Evolutionary Engineering." *Biotechnology for Biofuels* 6, no. 1: 89. https://doi.org/10.1186/1754-6834-6-89.

De Melo, H. F., B. M. Bonini, J. Thevelein, D. A. Simões, and M. A. Morais. 2010. "Physiological and Molecular Analysis of the Stress Response of *Saccharomyces cerevisiae* Imposed by Strong Inorganic Acid With Implication to Industrial Fermentations." *Journal of Applied Microbiology* 109, no. 1: 116–127. https://doi.org/10.1111/J.1365-2672.2009.04633.X.

Devantier, R., B. Scheithauer, S. G. Villas-Bôas, S. Pedersen, and L. Olsson. 2005. "Metabolite Profiling for Analysis of Yeast Stress Response During Very High Gravity Ethanol Fermentations." *Biotechnology and Bioengineering* 90, no. 6: 703–714. https://doi.org/10.1002/BIT.20457.

Entian, K. D., and P. Kötter. 2007. "25 Yeast Genetic Strain and Plasmid Collections." *Methods in Microbiology* 36: 629–666. https://doi.org/10.1016/S0580-9517(06)36025-4.

Franchi, M. A., G. E. Serra, and M. Cristianini. 2003. "The Use of Biopreservatives in the Control of Bacterial Contaminants of Sugarcane Alcohol Fermentation." *Journal of Food Science* 68, no. 7: 2310–2315. https://doi.org/10.1111/J.1365-2621.2003.TB05764.X.

Fukuda, N. 2023. "Apparent Diameter and Cell Density of Yeast Strains With Different Ploidy." *Scientific Reports* 13, no. 1: 1513. https://doi.org/10.1038/s41598-023-28800-z.

Gao, Y., S. Ray, S. Dai, et al. 2016. "Combined Metabolomics and Proteomics Reveals Hypoxia as a Cause of Lower Productivity on Scale-Up to a 5000-Liter CHO Bioprocess." *Biotechnology Journal* 11, no. 9: 1190–1200. https://doi.org/10.1002/BIOT.201600030.

Gasperotti, A., S. Brameyer, F. Fabiani, and K. Jung. 2020. "Phenotypic Heterogeneity of Microbial Populations Under Nutrient Limitation." *Current Opinion in Biotechnology* 62: 160–167. https://doi.org/10.1016/J.COPBIO.2019.09.016.

Gulli, J., E. Cook, E. Kroll, A. Rosebrock, A. Caudy, and F. Rosenzweig. 2019. "Diverse Conditions Support Near-Zero Growth in Yeast: Implications for the Study of Cell Lifespan." *Microbial Cell* 6, no. 9: 397–413. https://doi.org/10.15698/MIC2019.09.690.

Haringa, C. 2023. "An Analysis of Organism Lifelines in an Industrial Bioreactor Using Lattice-Boltzmann CFD." *Engineering in Life Sciences* 23, no. 1: e2100159. https://doi.org/10.1002/ELSC.202100159.

Haringa, C., A. T. Deshmukh, R. F. Mudde, and H. J. Noorman. 2017. "Euler-Lagrange Analysis Towards Representative Down-Scaling of a 22 m^3 Aerobic *S. cerevisiae* Fermentation." *Chemical Engineering Science* 170: 653–669. https://doi.org/10.1016/j.ces.2017.01.014.

Haringa, C., R. F. Mudde, and H. J. Noorman. 2018. "From Industrial Fermentor to CFD-Guided Downscaling: What Have We Learned?" *Biochemical Engineering Journal* 140: 57–71. https://doi.org/10.1016/J.BEJ.2018.09.001.

Haringa, C., W. Tang, A. T. Deshmukh, et al. 2016. "Euler-Lagrange Computational Fluid Dynamics for (Bio)Reactor Scale Down: An Analysis of Organism Lifelines." *Engineering in Life Sciences* 16, no. 7: 652–663. https://doi.org/10.1002/ELSC.201600061.

Haringa, C., W. Tang, G. Wang, et al. 2018. "Computational Fluid Dynamics Simulation of an Industrial *P. chrysogenum* Fermentation With a Coupled 9-Pool Metabolic Model: Towards Rational Scale-Down and Design Optimization." *Chemical Engineering Science* 175: 12–24. https://doi.org/10.1016/J.CES.2017.09.020.

Henrion, L., J. A. Martinez, V. Vandenbroucke, et al. 2023. "Fitness Cost Associated With Cell Phenotypic Switching Drives Population Diversification Dynamics and Controllability." *Nature Communications* 14, no. 1: 6128. https://doi.org/10.1038/s41467-023-41917-z.

Ho, P., S. Täuber, B. Stute, A. Grünberger, and E. von Lieres. 2022. "Microfluidic Reproduction of Dynamic Bioreactor Environment Based on Computational Lifelines." *Frontiers in Chemical Engineering* 4: 826485. https://doi.org/10.3389/FCENG.2022.826485.

Kapteyn, J. C., B. Ter Riet, E. Vink, et al. 2001. "Low External pH Induces *HOG1*-Dependent Changes in the Organization of the *Saccharomyces cerevisiae* Cell Wall." *Molecular Microbiology* 39, no. 2: 469–480. https://doi.org/10.1046/J.1365-2958.2001.02242.X.

Lara, A. R., E. Galindo, O. T. Ramírez, and L. A. Palomares. 2006. "Living With Heterogeneities in Bioreactors: Understanding the Effects of Environmental Gradients on Cells." *Molecular Biotechnology* 34, no. 3: 355–382. https://doi.org/10.1385/MB:34:3:355.

Larsson, G., M. Törnkvist, E. Wernersson, C. Trågårdh, H. Noorman, and S. O. Enfors. 1996. "Substrate Gradients in Bioreactors: Origin and Consequences." *Bioprocess Engineering* 14, no. 6: 281–289. https://doi.org/10.1007/BF00369471.

Lino, F. S. O., T. O. Basso, and M. O. A. Sommer. 2018. "A Synthetic Medium to Simulate Sugarcane Molasses." *Biotechnology for Biofuels* 11, no. 1: 221. https://doi.org/10.1186/S13068-018-1221-X.

Maeta, K., S. Izawa, S. Okazaki, S. Kuge, and Y. Inoue. 2004. "Activity of the Yap1 Transcription Factor in *Saccharomyces cerevisiae* Is Modulated by Methylglyoxal, a Metabolite Derived From Glycolysis." *Molecular and Cellular Biology* 24, no. 19: 8753–8764. https://doi.org/10.1128/MCB.24.19.8753-8764.2004.

Maier, A., B. Völker, E. Boles, and G. F. Fuhrmann. 2002. "Characterisation of Glucose Transport in *Saccharomyces cerevisiae* With Plasma Membrane Vesicles (Countertransport) and Intact Cells (Initial Uptake) With Single Hxt1, Hxt2, Hxt3, Hxt4, Hxt6, Hxt7 or Gal2 Transporters." *FEMS Yeast Research* 2, no. 4: 539–550. https://doi.org/10.1111/J.1567-1364.2002.TB00121.X.

Makanjuola, D. B., A. Tymon, and D. G. Springham. 1992. "Some Effects of Lactic Acid Bacteria on Laboratory-Scale Yeast Fermentations." *Enzyme and Microbial Technology* 14, no. 5: 350–357. https://doi.org/10.1016/0141-0229(92)90002-6.

Minden, S., M. Aniolek, H. Noorman, and R. Takors. 2023a. "Mimicked Mixing-Induced Heterogeneities of Industrial Bioreactors Stimulate Long-Lasting Adaption Programs in Ethanol-Producing Yeasts." *Genes* 14, no. 5. https://doi.org/10.3390/GENES14050997.

Minden, S., M. Aniolek, H. Noorman, and R. Takors. 2023b. "Performing In Spite of Starvation: How *Saccharomyces cerevisiae* Maintains Robust Growth When Facing Famine Zones in Industrial Bioreactors." *Microbial Biotechnology* 16, no. 1: 148. https://doi.org/10.1111/1751-7915.14188.

Minden, S., M. Aniolek, C. Sarkizi Shams Hajian, et al. 2022. "Monitoring Intracellular Metabolite Dynamics in *Saccharomyces cerevisiae* During Industrially Relevant Famine Stimuli." *Metabolites* 12, no. 3: 263. https://doi.org/10.3390/METABO12030263.

Nadai, C., G. Crosato, A. Giacomini, and V. Corich. 2021. "Different Gene Expression Patterns of Hexose Transporter Genes Modulate Fermentation Performance of Four *Saccharomyces cerevisiae* Strains." *Fermentation* 7, no. 3: 164. https://doi.org/10.3390/FERMENTATION7030164.

Nadal-Rey, G., D. D. McClure, J. M. Kavanagh, S. Cornelissen, D. F. Fletcher, and K. V. Gernaey. 2021. "Understanding Gradients in Industrial Bioreactors." *Biotechnology Advances* 46: 107660. https://doi.org/10.1016/J.BIOTECHADV.2020.107660.

Narendranath, N. V., S. H. Hynes, K. C. Thomas, and W. M. Ingledew. 1997. "Effects of Lactobacilli on Yeast-Catalyzed Ethanol Fermentations." *Applied and Environmental Microbiology* 63, no. 11: 4158–4163. https://doi.org/10.1128/AEM.63.11.4158-4163.1997.

Narendranath, N. V., and R. Power. 2005. "Relationship Between pH and Medium Dissolved Solids in Terms of Growth and Metabolism

of Lactobacilli and *Saccharomyces cerevisiae* During Ethanol Production." *Applied and Environmental Microbiology* 71, no. 5: 2239–2243. https://doi.org/10.1128/AEM.71.5.2239-2243.2005.

Neubauer, P., and S. Junne. 2016. "Scale-Up and Scale-Down Methodologies for Bioreactors." In *Bioreactors: Design, Operation and Novel Applications*, 323–354. Wiley-VCH Verlag GmbH. https://doi.org/10.1002/9783527683369.CH11.

Nguyen, J., J. Lara-Gutiérrez, and R. Stocker. 2021. "Environmental Fluctuations and Their Effects on Microbial Communities, Populations and Individuals." *FEMS Microbiology Reviews* 45, no. 4: 1–16. https://doi.org/10.1093/FEMSRE/FUAA068.

Nijkamp, J. F., M. van den Broek, E. Datema, et al. 2012. "De Novo Sequencing, Assembly and Analysis of the Genome of the Laboratory Strain *Saccharomyces cerevisiae* CEN.PK113-7D, a Model for Modern Industrial Biotechnology." *Microbial Cell Factories* 11, no. 1: 36. https://doi.org/10.1186/1475-2859-11-36.

Olsson, L., P. Rugbjerg, L. Torello Pianale, and C. Trivellin. 2022. "Robustness: Linking Strain Design to Viable Bioprocesses." *Trends in Biotechnology* 40, no. 8: 918–931. https://doi.org/10.1016/J.TIBTECH.2022.01.004.

Onetto, C. A., A. R. Borneman, and S. A. Schmidt. 2021. "Strain-Specific Responses by *Saccharomyces cerevisiae* to Competition by Non-*Saccharomyces* Yeasts." *Fermentation* 7, no. 3: 165. https://doi.org/10.3390/FERMENTATION7030165.

Ortega, A. D., V. Takhaveev, S. R. Vedelaar, et al. 2021. "A Synthetic RNA-Based Biosensor for Fructose-1,6-Bisphosphate That Reports Glycolytic Flux." *Cell Chemical Biology* 28: 1554–1568.e8. https://doi.org/10.1016/j.chembiol.2021.04.006.

Pereira, F. B., A. Romaní, H. A. Ruiz, J. A. Teixeira, and L. Domingues. 2014. "Industrial Robust Yeast Isolates With Great Potential for Fermentation of Lignocellulosic Biomass." *Bioresource Technology* 161: 192–199. https://doi.org/10.1016/J.BIORTECH.2014.03.043.

Pfeiffer, T., and A. Morley. 2014. "An Evolutionary Perspective on the Crabtree Effect." *Frontiers in Molecular Biosciences* 1: 17. https://doi.org/10.3389/fmolb.2014.00017.

Pianale, L. T., and L. Olsson. 2023. "ScEnSor Kit for *Saccharomyces cerevisiae* Engineering and Biosensor-Driven Investigation of the Intracellular Environment." *ACS Synthetic Biology* 12, no. 8: 2493–2497. https://doi.org/10.1021/ACSSYNBIO.3C00124.

Pinheiro, S., S. Pandey, and S. Pelet. 2022. "Cellular Heterogeneity: Yeast-Side Story." *Fungal Biology Reviews* 39: 34–45. https://doi.org/10.1016/J.FBR.2021.11.005.

Powell, C., D. Quain, and K. Smart. 2003. "The Impact of Brewing Yeast Cell Age on Fermentation Performance, Attenuation and Flocculation." *FEMS Yeast Research* 3, no. 2: 149–157. https://doi.org/10.1016/S1567-1356(03)00002-3.

R Core Team. 2020. *R: A Language and Environment for Statistical Computing*. R Foundation for Statistical Computing. https://www.r-project.org/.

Ribeiro, R. A., N. Bourbon-Melo, and I. Sá-Correia. 2022. "The Cell Wall and the Response and Tolerance to Stresses of Biotechnological Relevance in Yeasts." *Frontiers in Microbiology* 13: 953479. https://doi.org/10.3389/FMICB.2022.953479.

Sarkizi Shams Hajian, C., C. Haringa, H. Noorman, and R. Takors. 2020. "Predicting By-Product Gradients of Baker's Yeast Production at Industrial Scale: A Practical Simulation Approach." *Processes* 8, no. 12: 1554. https://doi.org/10.3390/pr8121554.

Schindelin, J., I. Arganda-Carreras, E. Frise, et al. 2012. "Fiji: An Open-Source Platform for Biological-Image Analysis." *Nature Methods* 9, no. 7: 676–682. https://doi.org/10.1038/nmeth.2019.

Schmidt, U., M. Weigert, C. Broaddus, and G. Myers. 2018. "Cell Detection With Star-Convex Polygons." *Lecture Notes in Computer Science (Including Subseries Lecture Notes in Artificial Intelligence and Lecture Notes in Bioinformatics)* 11071: 265–273. https://doi.org/10.1007/978-3-030-00934-2_30.

Shamir, M., Y. Bar-On, R. Phillips, and R. Milo. 2016. "SnapShot: Timescales in Cell Biology." *Cell* 164, no. 6: 1302–1302.e1. https://doi.org/10.1016/J.CELL.2016.02.058.

Spann, R., J. Glibstrup, K. Pellicer-Alborch, et al. 2019. "CFD Predicted pH Gradients in Lactic Acid Bacteria Cultivations." *Biotechnology and Bioengineering* 116, no. 4: 769–780. https://doi.org/10.1002/BIT.26868.

Takaine, M. 2019. "QUEEN-Based Spatiotemporal ATP Imaging in Budding and Fission Yeast." *Bio-Protocol* 9, no. 15: e3320. https://doi.org/10.21769/BIOPROTOC.3320.

Takors, R. 2012. "Scale-Up of Microbial Processes: Impacts, Tools and Open Questions." *Journal of Biotechnology* 160, no. 1–2: 3–9. https://doi.org/10.1016/J.JBIOTEC.2011.12.010.

Täuber, S., L. Blöbaum, V. Steier, M. Oldiges, and A. Grünberger. 2022. "Microfluidic Single-Cell Scale-Down Bioreactors: A Proof-of-Concept for the Growth of *Corynebacterium glutamicum* at Oscillating pH Values." *Biotechnology and Bioengineering* 119: 3194–3209. https://doi.org/10.1002/BIT.28208.

Täuber, S., C. Golze, P. Ho, E. Von Lieres, and A. Grünberger. 2020. "dMSCC: A Microfluidic Platform for Microbial Single-Cell Cultivation of *Corynebacterium glutamicum* Under Dynamic Environmental Medium Conditions." *Lab on a Chip* 20, no. 23: 4442–4455. https://doi.org/10.1039/D0LC00711K.

Thevelein, J. M. 1984. "Regulation of Trehalose Mobilization in Fungi." *Microbiological Reviews* 48, no. 1: 42–59. https://doi.org/10.1128/MR.48.1.42-59.1984.

Thomsson, E., C. Larsson, E. Albers, A. Nilsson, C. J. Franzén, and L. Gustafsson. 2003. "Carbon Starvation Can Induce Energy Deprivation and Loss of Fermentative Capacity in *Saccharomyces cerevisiae*." *Applied and Environmental Microbiology* 69, no. 6: 3251–3257. https://doi.org/10.1128/AEM.69.6.3251-3257.2003.

Torello Pianale, L., F. Caputo, and L. Olsson. 2023. "Four Ways of Implementing Robustness Quantification in Strain Characterisation." *Biotechnology for Biofuels and Bioproducts* 16, no. 1: 195. https://doi.org/10.1186/S13068-023-02445-6.

Torello Pianale, L., P. Rugbjerg, and L. Olsson. 2022. "Real-Time Monitoring of the Yeast Intracellular State During Bioprocesses With a Toolbox of Biosensors." *Frontiers in Microbiology* 12: 4220. https://doi.org/10.3389/FMICB.2021.802169.

Trivellin, C., L. Olsson, and P. Rugbjerg. 2022. "Quantification of Microbial Robustness in Yeast." *ACS Synthetic Biology* 11, no. 4: 1686–1691. https://doi.org/10.1021/acssynbio.1c00615.

Trivellin, C., P. Rugbjerg, and L. Olsson. 2024. "Performance and Robustness Analysis Reveals Phenotypic Trade-Offs in Yeast." *Life Science Alliance* 7, no. 1: e202302215. https://doi.org/10.26508/LSA.202302215.

Turner, J. J., J. C. Ewald, and J. M. Skotheim. 2012. "Cell Size Control in Yeast." *Current Biology* 22, no. 9: R350–R359. https://doi.org/10.1016/J.CUB.2012.02.041.

von Chamier, L., R. F. Laine, and J. Jukkala, et al. 2021. "Democratising Deep Learning for Microscopy With ZeroCostDL4Mic." *Nature Communications* 12, no. 1: 2276. https://doi.org/10.1038/s41467-021-22518-0.

Wehrs, M., D. Tanjore, T. Eng, J. Lievense, T. R. Pray, and A. Mukhopadhyay. 2019. "Engineering Robust Production Microbes for Large-Scale Cultivation." *Trends in Microbiology* 27, no. 6: 524–537. https://doi.org/10.1016/j.tim.2019.01.006.

Whitesides, G. M. 2006. "The Origins and the Future of Microfluidics." *Nature* 442, no. 7101: 368–373. https://doi.org/10.1038/nature05058.

Wucherpfennig, T., T. Hestler, and R. Krull. 2011. "Morphology Engineering – Osmolality and Its Effect on *Aspergillus niger* Morphology

and Productivity." *Microbial Cell Factories* 10, no. 1: 58. https://doi.org/10.1186/1475-2859-10-58.

Zhang, J., N. Sonnenschein, T. P. B. Pihl, K. R. Pedersen, M. K. Jensen, and J. D. Keasling. 2016. "Engineering an NADPH/NADP+ Redox Biosensor in Yeast." *ACS Synthetic Biology* 5, no. 12: 1546–1556. https://doi.org/10.1021/acssynbio.6b00135.

Zhang, N., and L. Cao. 2017. "Starvation Signals in Yeast Are Integrated to Coordinate Metabolic Reprogramming and Stress Response to Ensure Longevity." *Current Genetics* 63, no. 5: 839–843. https://doi.org/10.1007/S00294-017-0697-4.

Zieringer, J., M. Wild, and R. Takors. 2021. "Data-Driven In Silico Prediction of Regulation Heterogeneity and ATP Demands of *Escherichia coli* in Large-Scale Bioreactors." *Biotechnology and Bioengineering* 118, no. 1: 265–278. https://doi.org/10.1002/BIT.27568.

Supporting Information

Additional supporting information can be found online in the Supporting Information section.